J|A|C|S
ARTICLES
Published on Web 10/28/2005

An Anion-Dependent Switch in Selectivity Results from a Change of C−H Activation Mechanism in the Reaction of an Imidazolium Salt with $IrH_5(PPh_3)_2$

Leah N. Appelhans,[†] Daniele Zuccaccia,[‡] Anes Kovacevic,[†] Anthony R. Chianese,[†] John R. Miecznikowski,[†] Alceo Macchioni,[‡] Eric Clot,[§] Odile Eisenstein,*[,§] and Robert H. Crabtree*[,†]

Contribution from the Department of Chemistry, 225 Prospect Street, Yale University, New Haven, Connecticut 06520-8107, Dipartimento di Chimica, Università di Perugia, Via Elce di Sotto 8, 06123, Perugia, Italy, and LSDSMS (UMR 5636 CNRS), cc 14, Institut Gerhardt, Université Montpellier 2, F-34095 Montpellier Cedex 5, France

Received August 4, 2005; E-mail: robert.crabtree@yale.edu; eisenst@univ-montp2.fr

Abstract: Changing the counteranion along the series Br, BF_4, PF_6, SbF_6 in their ion-paired 2-pyridylmethyl imidazolium salts causes the kinetic reaction products with $IrH_5(PPh_3)_2$ to switch from chelating *N*-heterocyclic carbenes (NHCs) having normal C2 (N path) to abnormal C5 binding (AN path). Computational work (DFT) suggests that the AN path involves C−H oxidative addition to Ir^{III} to give Ir^{V} with little anion dependence. The N path, in contrast, goes by heterolytic C−H activation with proton transfer to the adjacent hydride. The proton that is transferred is accompanied by the counteranion in an anion-coupled proton transfer, leading to an anion dependence of the N path, and therefore of the N/AN selectivity. The N path goes via Ir^{III}, not Ir^{V}, because the normal NHC is a much less strong donor ligand than the abnormal NHC. PGSE NMR experiments support the formation of ion-pair in both the reactants and the products. $^{19}F,^{1}H$-HOESY NMR experiments indicate an ion-pair structure for the products that is consistent with the computational prediction (ONIOM(B3PW91/UFF)).

Introduction

Counterion effects resulting from ion-pairing (IP) have recently taken a more prominent role in organometallic chemistry.[1] Some of us have applied ^{1}H NOESY and $^{19}F,^{1}H$-HOESY NMR spectroscopy to the investigation of predominant ion-pair solution structures of organometallic complexes by the detection of interionic contacts.[2−4] We have shown that the solution ion-pair structures can be predicted by ONIOM (B3PW91/UFF) calculations of the ion-pair geometry.[5,6] The results suggest that these ion-pairs have surprisingly well-defined structures. Although absolute IP energies can be large, only differences in this energy with change of anion can lead to any experimentally observable counterion-dependent switching of reaction pathway in solution. Even then, the two transition states (TS) involved in any two such competing reactions need to be close in energy. For asymmetric catalysis, this condition is automatically fulfilled and several cases of anion-dependent effects on ee have been reported.[7,8] In this context, Lacour has seen IP effects in asymmetric anions,[9] and the importance of ion-pair formation in the kinetics of deprotonation of dihydrogen complexes has been studied by calculations.[10]

In this paper, we report in full on strong counterion effects in the reaction of 2-pyridylmethyl imidazolium salts with $IrH_5(PPh_3)_2$ to give chelating[11,12] NHC[13−18] complexes; depending on the anion, the NHCs can be bound either at C2 or at C5.[19] With anions such as bromide, capable of strong IP by C−H···Br hydrogen bonding at C2,[20] the normal C2 NHC is

[†] Yale University.
[‡] Università di Perugia.
[§] Université Montpellier 2.

(1) Macchioni, A. *Chem. Rev.* **2005**, *105*, 2039 and references therein.
(2) Bellachioma, G.; Cardaci, G.; Macchioni, A.; Reichenbach, G.; Terenzi, S. *Organometallics* **1996**, *15*, 4349.
(3) Macchioni, A.; Bellachioma, G.; Cardaci, G.; Gramlich, V.; Rüegger, H.; Terenzi, S.; Venanzi, L. M. *Organometallics* **1997**, *16*, 2139.
(4) Macchioni, A. *Eur. J. Inorg. Chem.* **2003**, 195.
(5) Macchioni, A.; Zuccaccia, C.; Clot, E.; Gruet, K.; Crabtree, R. H. *Organometallics* **2001**, *20*, 2367.
(6) Gruet, K.; Clot, E.; Eisenstein, O.; Lee, D.-H.; Patel, B.; Macchioni, A.; Crabtree, R. H. *New J. Chem.* **2003**, *27*, 80.
(7) Pfaltz, A.; Blankenstein, J.; Hilgraf, R.; Hörmann, E.; McIntrye, S.; Menges, F.; Schönleber, M.; Smidt, S. P.; Wüstenberg, B.; Zimmermann, N. *Adv. Synth. Catal.* **2003**, *345*, 33.
(8) Llewellyn, D. B.; Adamson, D.; Arndtsen, B. A. *Org. Lett.* **2000**, *2*, 4165.
(9) Lacour, J.; Hebbe-Viton, V. *Chem. Soc. Rev.* **2003**, 373.
(10) Basallote, M. G.; Besora, M.; Durán, J.; Fernández-Trujillo, M. J.; Lledós, A.; Máñez, M. A.; Maseras, F. *J. Am. Chem. Soc.* **2004**, *126*, 2320.
(11) Peris, E.; Loch, J. A.; Mata, J.; Crabtree, R. H. *Chem. Commun.* **2001**, 201.
(12) Peris, E.; Crabtree, R. H. *Coord. Chem. Rev.* **2004**, *248*, 2239.
(13) Bourissou, D.; Guerret, O.; Gabbai, F. P.; Bertrand, G. *Chem. Rev.* **2000**, *100*, 39.
(14) Herrmann, W. A.; Reisinger, C. P.; Spiegler, M. *J. Organomet. Chem.* **1998**, *557*, 93.
(15) Herrmann, W. A. *Angew. Chem., Int. Ed.* **2002**, *41*, 1291.
(16) Ho, V. M.; Watson, L. A.; Huffman, J. C.; Caulton, K. G. *New J. Chem.* **2003**, *27*, 1446.
(17) Grudden, C. M.; Allen, D. P. *Coord. Chem. Rev.* **2004**, *248*, 2247.
(18) Cavell, K. J.; McGuinness, D. S. *Coord. Chem. Rev.* **2004**, *248*, 671.
(19) Kovacevic, A.; Gründemann, S.; Miecznikowski, J. R.; Clot, E.; Eisenstein, O.; Crabtree, R. H. *Chem. Commun.* **2002**, 2580.
(20) Sambrook, M. R.; Beer, P. D.; Wisner, J. A.; Paul, R. L.; Cowley, A. R.; Szemes, F.; Drew, M. G. B. *J. Am. Chem. Soc.* **2005**, *127*, 2292 and references therein.

Table 1. Ratio of **2** to **3** for Various R and A in Eq 1

	R	A	**2** (normal)	**3** (abnormal)
a	Me	Br	91	9
b	Me	OAc	80	20
c	Me	OCOAr[a]	70	30
d	Me	BF_4	45	55
e	Me	PF_6	50	50
f	Me	OCOPh	50	50
g	Me	SbF_6	11	89
h	*i*-Pr	Br	84	16
i	*i*-Pr	BF_4	0	100
j	*n*-Bu	BF_4	5	95

[a] O_2CAr = 2,4,6-triisopropylbenzoate.

obtained (N path), while changing the counterions along the series Br, BF_4, PF_6, SbF_6 progressively switches the kinetic product to the abnormal C5 species (AN path). Such C5 NHCs are still rare, but several other examples have now been reported.[21−23]

Formation of NHCs by C−H oxidative addition was proposed some years ago,[24] but this pathway was only authenticated recently by Peris *et al.* who observed the oxidative addition product directly.[25] Previous computational (DFT) work has analyzed the bonding associated with the NHC−metal interaction.[26−32] Few examples have yet been reported on the pathways by which NHC complexes are formed by reaction of parent imidazolium salts with metal complexes.[25,33,34] We now find that such calculations have allowed us to understand the anion effect as a result of the N and AN paths having different mechanisms with different sensitivities to the nature of the anion.

Results and Discussion

(1) Experimental and Theoretical Studies of the Ion-Pair Structures. NHCs are attracting attention in organometallic chemistry,[13,14] but improved synthetic routes are sought for metallating the precursor imidazolium salts. The harsh conditions of the early work (e.g., BuLi) are not compatible with the functionality-rich NHCs that are increasingly employed.[35] We therefore attempted metalation via reaction of a metal hydride, $[IrH_5(PPh_3)_2]$, with the imidazolium salt **1i** (R = *i*-Pr, A = BF_4; see Table 1 for the numbering scheme) with the result that the NHC was obtained, accompanied by loss of H_2.[36] Instead of the normal C2 NHC, however, the abnormal C5 isomer was obtained. The normal isomer could still be obtained if the C4 and C5 positions were blocked, as in the benzimidazolium salts. For small wingtip groups at N3, such as methyl, a mixture of normal (**2**) and abnormal (**3**) NHCs was seen (Table 1). For example, the reaction of eq 1 (R = Me, A = BF_4) gave a 45:55 ratio of products **2d** and **3d** (R = Me, A = BF_4).

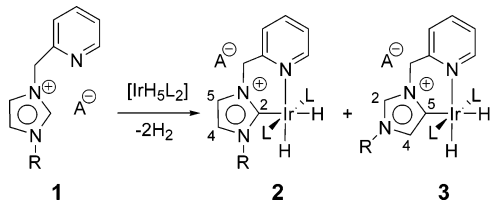

(1)

The product ratio is kinetic because the **2**/**3** ratio is invariant on subsequent change of the anion. Thermal interconversion of **2** and **3** was never seen even after prolonged reactions times. For example, the 45:55 mixture from **1d** (R = Me, A = BF_4) can be converted either to the Br or to the SbF_6 salt by ion exchange. The products retain the 45:55 ratio of the starting material even on heating (5 h, refluxing thf). The ion present during the synthesis therefore decides the ratio, not any anion subsequently introduced.

The abnormal isomer was obtained in pure form by synthesis with the BF_4 salt, followed by recrystallization, and fully characterized. The normal isomer was obtained in pure form from the imidazolium salt and $[IrH_2(Me_2CO)_2L_2]BF_4$ (see Experimental Section). The very different spectroscopic characteristics of the two types of NHC, fully discussed previously by comparison with crystallographically authenticated examples, allows secure identification even in mixtures.[36] In particular, the adjacent imidazole C4 and C5 aromatic protons of normal isomer **2d** are relatively close in proton NMR chemical shift ($CDCl_3$), δ 7.44 and 6.31, as expected on the basis of prior work, while the nonadjacent aromatic protons of abnormal **3d**, C2 and C4, are more separated, δ 8.66 and 4.88, again as expected. The particularly downfield shift of the C2 proton is consistent with its acidic character. Also in line with previous data, the C2 carbene carbon has a lower field ^{13}C NMR chemical shift, ($CHCl_3$) 169.9 ppm (BF_4 salt), than the C5 carbene, 142.0 ppm (BF_4 salt).

While complex **2** was not converted to **3** nor vice versa thermally under neutral conditions, even after anion exchange, HBF_4/CH_2Cl_2 treatment at room temperature completely converts **3** to **2**, so **2** is the thermodynamically more stable product. This confirms that, although the energies of **2** and **3** may be close, any abnormal product **3** formed in eq 1 is entirely a kinetic product. This acid treatment is also a method for obtaining the normal isomers in pure form.

We looked at the effect on eq 1 of variation of the anion, A, prompted by computational work, detailed below, that suggested that the energetics of the system **2**/**3** are dependent on the anion. The results of the reaction of eq 1 for a series of anions and wingtip groups are shown in Table 1. Moving to less strongly ion-pairing and bulkier counterions along the IP effect series Br > OAc > BF_4 > PF_6 > SbF_6 progressively switches the kinetic product from the normal C2 to the abnormal C5 species. For a fixed anion, the more bulky R group, ^{i}Pr, leads to the less hindered abnormal NHC being relatively favored versus

(21) Lebel, H.; Janes, M. K.; Charette, A. B.; Nolan, S. P. *J. Am. Chem. Soc.* **2004**, *126*, 5046.
(22) Danopoulos, A. A.; Tsoureas, N.; Wright, J. A.; Light, M. E. *Organometallics* **2004**, *23*, 166.
(23) Hu, X.; Castro-Rodriguez, I.; Meyer, K. *Organometallics* **2003**, *22*, 3016.
(24) (a) McGuinness, D. S.; Cavell, K. J.; Yates, B. F.; Skelton, B. W.; White, A. H. *J. Am. Chem. Soc.* **2001**, *123*, 8317. (b) McGuinness, D. S.; Saendig, N.; Yates, B. F.; Cavell, K. J. *J. Am. Chem. Soc.* **2001**, *123*, 4029. (c) Gründemann, S.; Albrecht, M.; Kovacevic, A.; Faller, J. W.; Crabtree, R. H. *Dalton Trans.* **2002**, 2163.
(25) Viciano, M.; Mas-Marza, E.; Poyatos, M.; Sanau, M.; Crabtree, R. H.; Peris, E. *Angew. Chem., Int. Ed.* **2005**, *44*, 444.
(26) Frenking, G.; Frohlich, N. *Chem. Rev.* **2000**, *100*, 717.
(27) Dorta, R.; Stevens, E. D.; Scott, N. M.; Costabile, C.; Cavallo, L.; Hoff, C. D.; Nolan, S. P. *J. Am. Chem. Soc.* **2005**, *127*, 2485.
(28) Perrin, L.; Clot, E.; Eisenstein, O.; Loch, J.; Crabtree, R. H. *Inorg. Chem.* **2001**, *40*, 5806.
(29) Baba, E.; Cundari, T. R.; Firkin, I. *Inorg. Chim. Acta* **2005**, 358.
(30) Mungur, S. A.; Liddle, S. T.; Wilson, C.; Sarsfield, M. J.; Arnold, P. J. *Chem. Commun.* **2004**, 2738.
(31) Hu, X. L.; Castro-Rodriguez, I.; Olsen, K.; Meyer, K. *Organometallics* **2004**, *23*, 755.
(32) Green, J. C.; Herbert, B. J. *Dalton Trans.* **2005**, 1214.
(33) Clement, N. D.; Cavell, K. J.; Jones, C.; Elsevier, C. J. *Angew. Chem., Int. Ed.* **2004**, *43*, 1277.
(34) McGuiness, D. S.; Cavell, K. J.; Yates, B. F. *Chem. Commun.* **2001**, 355.
(35) Rivera, G.; Crabtree, R. H. *J. Mol. Catal. A* **2004**, *222*, 59.
(36) Gründemann, S.; Kovacevic, A.; Albrecht, M.; Faller, J. W.; Crabtree, R. H. *J. Am. Chem. Soc.* **2002**, *124*, 10473.

the R = Me case (Table 1, entries **a** vs **h**, and **d** vs **i**, respectively). The magnitude of the effects seen here goes beyond the modest ones usual in organometallic chemistry, although larger anion effects have come to light more recently.[37] When equimolar quantities of the bromide (**1a**) and SbF_6 (**1g**) salts were employed, a 55:45 ratio of normal:abnormal resulted (R = Me). This suggests that each ion-pair reacts independently at similar rates.

The anion hydrogen bonded as C−H···A to the C2 position of the imidazolium reactant **1** might have been expected to sterically block reaction at that site. In the series Br > OAc > BF_4 > PF_6 > SbF_6, the steric and electronic factors reinforce each other: SbF_6 is both bulkier and less strongly ion-pairing than Br. Steric effects do operate in this system. If the methyl wingtip group is replaced by ^{i}Pr, the abnormal product is obtained with the weakly coordinating anion BF_4 (Table 1, entry **i**), an anion that previously gave 45:55 mixtures (Table 1, entry **d**). The larger ^{i}Pr group causes the reaction to favor the less hindered abnormal NHC. Only with Br is the normal compound seen, and then only in an 84:16 ratio (Table 1, entry **h**). The results for the three carboxylates (**b**, **c**, and **f**), particularly the contrast between $PhCO_2$ and the bulky $ArCO_2$, suggest that we have a combination of steric and electronic effects in this case.

NMR Studies of the Imidazolium Ion-Pair Solution Structure. The starting imidazolium salt has an ion-pair structure (see **1**) in which the anion is hydrogen bonded to the C2 proton, consistent with the present computational data (vide infra) and with literature expectations.[38] This is perhaps most easily shown by the sensitivity of the proton NMR shift of C2−H to the nature of the anion. For example, for the model imidazolium salt **4**, the resonance shifts ($CDCl_3$) are as follows: A = Br, δ 10.45; BF_4, 9.85; PF_6, 8.79; SbF_6, 8.50. The same interaction is detected in the abnormal carbene **3**, where the acidic CH is directed away from the metal. The range of shifts seen is very similar: A = Br, δ 9.71 (**3a**); BF_4, 8.66 (**3d**); PF_6, 8.44 (**3e**); SbF_6, 8.38 (**3g**). Bromide can readily replace SbF_6 (or BF_4) as ion-pairing partner in **4**, as shown by the change in chemical shift of the C2−H proton from that of the SbF_6 salt to that of the Br salt on addition of NBu_4Br in $CDCl_3$. The titration curve suggests K_{eq} is 1.6 in favor of Br. Similar ion-pairing effects in imidazolium salts have been reported.[38]

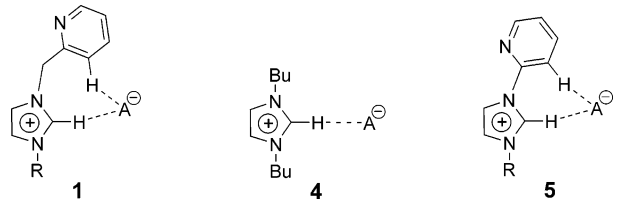

^{19}F,^{1}H-HOESY NMR spectra of **1i** (R = *i*-Pr and A = BF_4) and **5** (R = *i*-Pr and A = BF_4) pyridyl-imidazolium salts recorded in CD_2Cl_2 show strong dipolar interactions between the anion ^{19}F and cation 2, 13, 12, CH_2 (in the case of **1i**), and 11 ^{1}H nuclei (Figure S1 in Supporting Information). This indicates that the pyridine nitrogen is predominantly oriented in pseudo-trans position with respect to the anion. This apparent predisposition toward the formation of the abnormal carbene is not, however, the key factor (vide infra). The same prevalent orientation is observed in THF-d_8 for **1i** (R = *i*-Pr and A = BF_4) as that of the solvent used in the syntheses (Figure 1, left). A confirmation of the preferred orientation of the pyridine ring comes from the observation of 11/2 NOE intensity that is about 3 times that of 11/5 in the ^{1}H-NOESY NMR spectrum recorded for **5** (R = *i*-Pr and A = BF_4) in CD_2Cl_2 (Figure S2 in Supporting Information). The anion has a key role in determining the relative orientation of the pyridine to the imidazolium: in CD_3NO_2, where PGSE (pulsed field gradient spin−echo)[39,40] NMR experiments suggest the prevalence of free ions (Table S1 in Supporting Information), the intensities of the 11/2−11/5 NOEs almost invert (Figure S3 in Supporting Information), so there is now an apparent predisposition toward normal carbene.

NMR Studies of the Iridium Ion-Pair Solution Structure. The ion-pair structure of complexes **2i**, **2j**, **3i**, and **3j** was investigated in CD_2Cl_2 and THF-d_8 solution, where PGSE measurements show that the complexes are mainly present as intimate ion-pairs (Table S1 in Supporting Information). The greater solubility of the *n*-Bu and *i*-Pr analogues led to the choice of these derivatives for this part of the study. Dipolar interactions between anion ^{19}F and cation ^{1}H nuclei are detected in the ^{19}F,^{1}H-HOESY spectra. As shown from the NMR data in Figure 1 (right) obtained in exactly the same conditions as the synthesis, the F nuclei of the counteranion of complexes **3i** interact with 2, 12, 6, 14, *m*, and, likely, *o* (overlapped with 12) protons. No contact is observed with the two hydrides. The same interactions are also observed for both abnormal and normal complexes in CD_2Cl_2 (Figure S4 in Supporting Information). A response was also detected at the α position of the *n*-Bu wingtip group only in the abnormal case, where the R group projects into the region where the anion binds. A more detailed discussion of this NMR experiment is available for a closely related complex.[5]

Ion-Pair Structure−Computational. From the NMR studies on the products, the anion is essentially located in the vicinity of the most protonic C−H bond: C2−H for the abnormal and C5−H for the normal isomer. However, IP contacts were also seen with the protons of the methylene linker and with H12 on the pyridine ring. To better characterize the network of H-bonds operating in these systems, ONIOM (B3PW91/UFF) calculations were carried out. In the system chosen, the wingtip group is ^{i}Pr treated at the MM level (UFF) together with the phenyl groups on PPh_3, whereas the rest of the molecule, including the anion, is treated at the DFT (B3PW91) level. The anions considered are BF_4, Br, and OAc, and Figure 2 shows the optimized geometries for the normal (**N**) and abnormal (**AN**) carbenes, respectively. Selected geometrical parameters are given in Table 2.

In the absence of anion, the geometries of the normal (**N**) and abnormal (**AN**) isomers are very similar. The only

(37) Smidt, S. P.; Zimmermann, N.; Studer, M.; Pfaltz, A. *Chem.-Eur. J.* **2004**, *10*, 4685.
(38) Cowan, J. A.; Clyburne, J. A. C.; Davidson, M. G.; Harris, R. L. W.; Howard, J. A. K.; Küpper, P.; Leech, M. A.; Richards, S. P. *Angew. Chem., Int. Ed.* **2002**, *41*, 1432.
(39) (a) Hahn, E. L. *Phys. Rev.* **1950**, *80*, 580. (b) Stejskal, E. O.; Tanner, J. E. *J. Chem. Phys.* **1965**, *42*, 288. (c) Stilbs, P. *Prog. Nucl. Magn. Reson. Spectrosc.* **1987**, *19*, 1. (d) Price, W. S. *Concepts Magn. Reson.* **1997**, *9*, 299. (e) Price, W. S. *Concepts Magn. Reson.* **1998**, *10*, 197. (f) Johnson, C. S., Jr. *Prog. Nucl. Magn. Reson. Spectrosc.* **1999**, *34*, 203.
(40) For reviews on applications to organometallic chemistry, see: (a) Valentini, M.; Rüegger, H.; Pregosin, P. S. *Helv. Chim. Acta* **2001**, *84*, 2833. (b) Binotti, B.; Macchioni, A.; Zuccaccia, C.; Zuccaccia, D. *Comments Inorg. Chem.* **2002**, *23*, 417. (c) Pregosin, P. S.; Martinez-Viviente, E.; Kumar, P. G. A. *Dalton Trans.* **2003**, 4007.

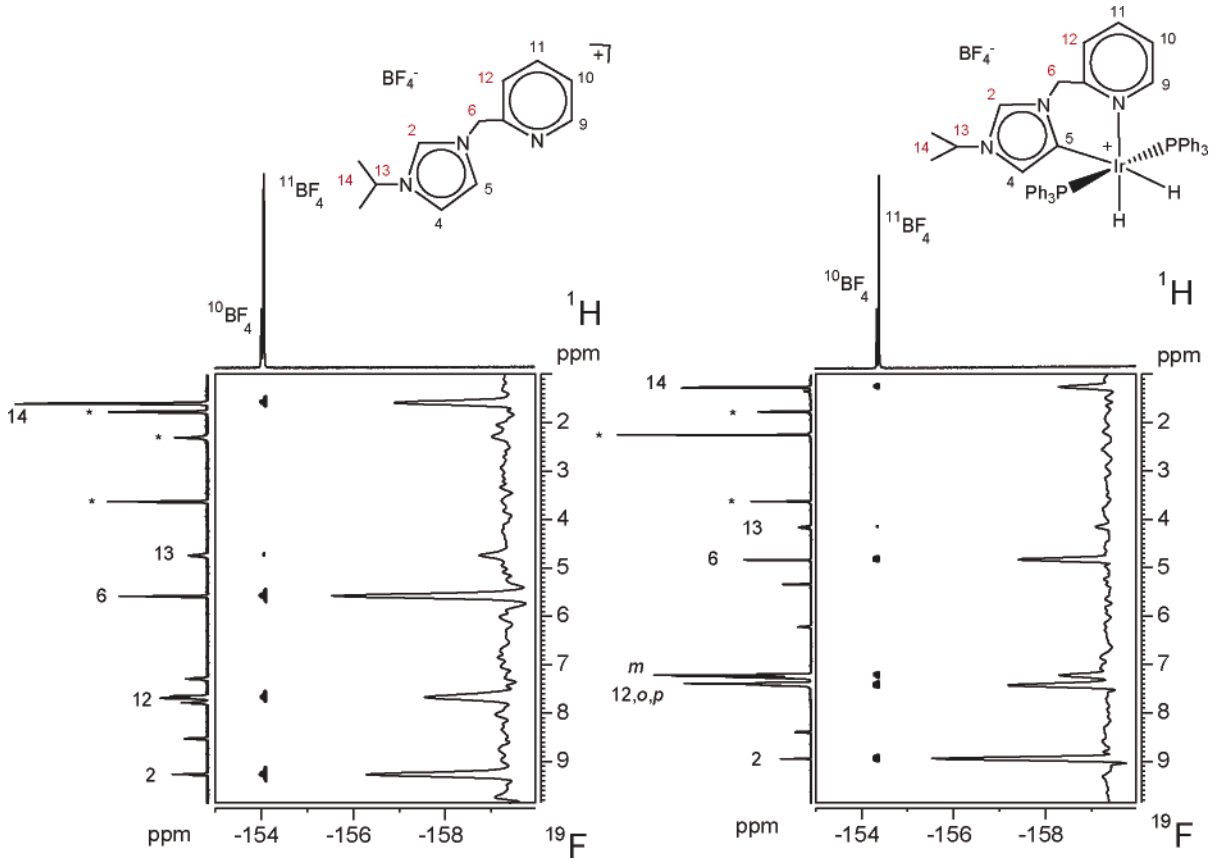

Figure 1. $^{19}F,^{1}H$-HOESY NMR spectra (376.65 MHz, 323 K, THF-d_8) of **1i** (left, R = *i*-Pr and A = BF_4) and **3i** (right, R = *i*-Pr and A = BF_4) showing the selective interactions of the anion with the indicated protons. "*" denotes THF and water resonances.

significant difference is the longer Ir−H_C[41] bond with the hydride trans to C5 in **AN** (1.623 Å) than trans to C2 in **N** (1.600 Å). The higher electron-donating power of the **AN** form[42] leads to a higher trans effect, also illustrated by the shorter Ir−C bond in **AN** (2.098 Å) than in **N** (2.115 Å). The C−H bond that is not activated has the same value in both isomers (1.079 Å), thus giving a reference for systems with anion interactions at this position.

Upon interaction with BF_4, the geometry of the two carbene isomers, **N-BF$_4$** and **AN-BF$_4$**, is slightly altered. The most significant change is the elongation of the C−H bond close to the anion (C5−H = 1.082 Å, **N-BF$_4$**; C2−H = 1.092 Å, **AN-BF$_4$**), clearly indicating the presence of H-bonding interactions with the latter. As expected, the effect is more pronounced for the more acidic C2−H bond. The interaction associated with BF_4 in **AN-BF$_4$** is also reflected by the elongation of the Ir−C5 bond (2.098 Å, **AN**; 2.107, **AN-BF$_4$**), whereas the Ir−N bond remains unchanged. This situation is not observed in **N-BF$_4$** where the Ir−C2 bond is left unchanged while the Ir−N bond shortens (2.239 Å, **N**; 2.219, **N-BF$_4$**). Several short contacts are observed between the anion and the cation (Table 2). For the normal isomer, the shortest contacts are with the hydrogen atom on the pyridine ring (2.109 Å) and bound to C5 (2.129 Å) consistent with both protons having similar acidity. A short contact is also obtained with the bridging methylene protons (2.053 Å). The BF_4 anion thus acts as a chelating, outer sphere ligand that can form H-bonds with several centers at once. These data are in full agreement with the NMR studies.

The higher acidity of the H atom bound to C2 in **AN-BF$_4$** induces a shift in the position of the BF_4 anion resulting in a shortened contact (1.820 Å) with C2−H and an elongated contact with the pyridine (2.147 Å). This shift is best illustrated by the increase in the Ir−C···B angle from 111.8° in **N-BF$_4$** to 123.7° in **AN-BF$_4$**.

We have also compared the contacts in **AN-BF$_4$** to those observed in the X-ray structure.[36,43] Because of the uncertainty in the location of the H atoms in the X-ray structure, we have considered F···C distances in the comparison. In the crystallographically characterized structure, the contacts with the pyridine and C2 are 3.189 and 3.507 Å, respectively. In the calculated structure **AN-BF$_4$**, the corresponding values are 2.895 and 3.133 Å, respectively. There is thus a qualitative agreement, even though the experimental values are longer, perhaps due to interaction of the anion with molecules of other unit cells. These results clearly indicate that the anion position, conserved both in the solid and in solution, is associated with the presence of a network of hydrogen bonds.

The nonchelating anion, Br, is less apt to form this network of hydrogen bonds because Br can at most only be involved in bifurcated H-bonds. The optimal geometries for **N-Br** and **AN-Br** (Figure 2) therefore reflect the best compromise between the various possible interactions. In the normal isomer **N-Br**, the pyridine and C5−H hydrogen atoms, having similar acidity,

(41) H_c refers to the hydride trans to the carbene ligand, and H_N refers to the hydride trans to pyridine in the product of C−H activation; see Table 2.
(42) Chianese, A. R.; Kovacevic, A.; Zeglis, B. M.; Faller, J. W.; Crabtree, R. H. *Organometallics* **2004**, *23*, 2461.
(43) Gründemann, S.; Kovacevic, A.; Albrecht, M.; Faller, J. W.; Crabtree, R. H. *Chem. Commun.* **2001**, 2274.

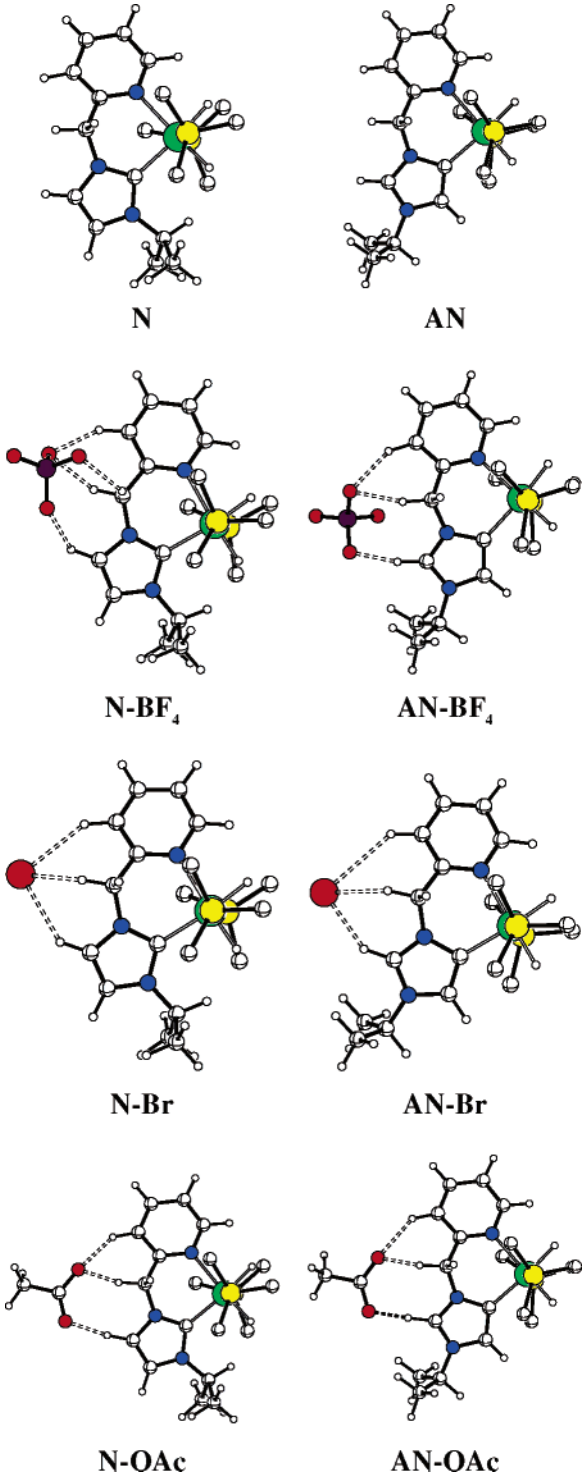

Figure 2. Optimized QM/MM geometries for normal (N) and abnormal (AN) carbene complexes in their ion-pairs with BF_4 (**N-BF$_4$** and **AN-BF$_4$**), Br (**N-Br** and **AN-Br**), and OAc (**N-OAc** and **AN-OAc**). For clarity, only the *ipso* PPh_3 carbons are shown.

adopt an intermediate geometry with long Br···H contacts, automatically giving a shorter contact with the linker CH_2 protons (Table 2). The C5−H elongation is slightly greater than that with BF_4 (1.085 Å, **N-Br**; 1.082 Å, **N-BF$_4$**), showing that, despite its remote position, Br is a better H-bond acceptor.

The greater acidity of C2−H in **AN** results in a shortening of the contact with the C2−H proton (2.422 Å) and a lengthening of that with the pyridine (3.059 Å). The C2−H bond is significantly elongated (1.097 vs 1.085 Å) as a result of stronger H-bonding. As observed with BF_4, the counteranion shifts closer to the imidazolium ion no doubt to enhance the preferred H-bonding interaction (Ir−C2···Br = 121.5°, **N-Br**; Ir−C5···Br = 124.5°, **AN-Br**). However, the Br anion still interacts with multiple Hs, not just with C2−H in a linear C2−H···Br hydrogen bond.

Moving to a chelating anion, acetate CH_3COO (OAc), allows interaction with a greater number of H atoms. In the normal isomer **N-OAc**, the very short contact with H−C5 (1.842 Å) indicates formation of a strong hydrogen bond. The C5−H bond is significantly more elongated (1.106 Å) than in the case of BF_4 (1.082 Å) or Br (1.085 Å). Also, the O···H−C5 atoms are almost collinear (170°) as expected for a classical hydrogen bond. Nevertheless, the chelating ability of OAc means that the formation of this strong H-bond is not made at the expense of the interaction with the equally acidic pyridine proton and the contact with pyridine is also the shortest among the series of normal isomers (2.109 Å, **N-BF$_4$**; 2.740 Å, **N-Br**; 2.019 Å, **N-OAc**).

In the abnormal isomer **AN-OAc**, the more acidic H−C2 center attracts the OAc so that the O···H−C2 contact is very short (1.659 Å) and the elongation of the H−C2 bond is very large (1.135 Å). In this case, almost perfect linearity is achieved (172.3°) as expected for a strong H-bond. A contact with the pyridine ring is still possible via the second oxygen atom with comparable distances (2.147 Å, **AN-BF$_4$**; 2.170 Å, **AN-OAc**).

This argument means that the intrinsic basicity of the anion is not the sole factor. The NMR data on **4** clearly demonstrate that Br is a better H-bond acceptor for H−C2 than BF_4, but in this system there was no competition with other protons of similar acidity (the butyl hydrogens are not so acidic). Therefore, the sole possibility is for the anion to engage in a hydrogen bond with the sole acidic proton, H−C2. For the pyridine-substituted ligand, the situation is more complex and the presence of the acidic pyridine protons allows for several H-bonding interactions with formation of a network of hydrogen bonds that can only be fully exploited by anions with several H-bonding sites (BF_4, OAc). Depending upon the IP architecture, this possibility for extra stabilization in chelating anions can lead to an inversion in the expected IP stabilization along a series versus that expected from anion basicity.

Ion-Pair Energetics−Computational. ONIOM(B3PW91/UFF) calculations show that the thermodynamic preference is always for the normal carbene isomer. The free normal NHC **1-N** proved to be 14.5 kcal mol^{-1} more stable than the abnormal isomer **1-AN**. Coordination to the Ir fragment reduced the difference to 10.1 kcal mol^{-1}, no doubt because the abnormal isomer is a stronger σ-donor as shown experimentally by reduced ν(CO) frequencies.[42] In full agreement with the creation of the network of H-bonding interactions discussed above, introduction of the anion causes a much larger reduction to 3.8 kcal mol^{-1} for Br, 1.6 kcal mol^{-1} for BF_4, and 0.9 kcal mol^{-1} for acetate (Table 3). The values reflect the efficiency with which the anion can interact with the full set of protons available in the imidazolium and pyridine rings as described previously. Thus, the nonchelating anion (Br) affords less extra stabilization for the abnormal isomer when compared to the strongly chelating H-bond acceptor, acetate. Modeling the CH_2Cl_2 solvent (CPCM continuum model) slightly increases the preference for

Table 2. Selected Geometric Parameters (Å) for the Various Complexes Optimized (H_N and H_C Refer to the Hydrides Trans to Pyridine and to the Carbene Carbon, Respectively)

	N	N-BF_4	N-Br	N-OAc	AN	AN-BF_4	AN-Br	AN-OAc
Ir−H_N	1.573	1.581	1.578	1.579	1.577	1.582	1.582	1.582
Ir−H_C	1.600	1.608	1.608	1.610	1.623	1.630	1.630	1.633
Ir−N	2.239	2.219	2.236	2.232	2.230	2.230	2.234	2.230
Ir−C2	2.115	2.114	2.121	2.121				
Ir−C5					2.098	2.107	2.109	2.109
Ir−P	2.327/2.393	2.331/2.371	2.316/2.386	2.316/2.380	2.326/2.367	2.314/2.360	2.316/2.359	2.313/2.357
C2−H					1.079	1.092	1.097	1.135
C5−H	1.079	1.082	1.085	1.106				
A···H2[a]						1.820	2.422	1.659
A···H5		2.129	2.771	1.842				
A···CH_2[b]		2.053	2.372	1.851		2.059	2.451	1.875
A···CH_{py}[c]		2.109	2.740	2.019		2.147	3.059	2.170

[a] These contacts between the anion and the cation correspond to the shortest distance in each case. [b] CH_2 denotes the methylene linker between pyridine and imidazole. [c] CH_{py} corresponds to the pyridine proton H12.

Table 3. Relative ONIOM(B3PW91/UFF) and CPCM(B3PW91/CH_2Cl_2) Energies (kcal mol^{-1}) of the Abnormal (**AN**, **AN-BF$_4$**, **AN-Br**, **AN-Ac**) with Respect to the normal (**N**, **N-BF$_4$**, **N-Br**, **N-Ac**) Carbene Complex[a]

			E_b[b]	
anion	ONIOM	CPCM	normal	abnormal
none	10.1	7.7		
BF_4	1.6	1.9	−8.4	−12.3
Br	3.8	5.7	−0.8	−3.6
CH_3COO	0.9	4.5	−11.5	−15.9

[a] The normal is always more stable. [b] The ion-pair binding energies E_b (kcal mol^{-1}) are evaluated for each isomer at the CPCM(B3PW91/CH_2Cl_2) level.

the normal isomer: 5.7 kcal mol^{-1} (Br), 4.5 kcal mol^{-1} (OAc), and 1.9 kcal mol^{-1} (BF_4). Nevertheless, inclusion of the solvent does not qualitatively alter the stabilizing effect of the anion.

We also estimated the ion-pair interaction energy with CPCM calculations. The ion-pair ONIOM geometries were used in three different CPCM calculations: ion-pair, cation, and anion. From the three energies obtained at the B3PW91 level within the CPCM scheme, the interaction energy E_b was computed as E(ion-pair) − {E(cation) + E(anion)}. The negative values obtained (Table 3) indicate a stabilizing tendency for the ion-pair in agreement with NOE and PGSE NMR observations. The interaction energies are smaller when the anion interacts with the less acidic H−C5. Interestingly, as anticipated from the analysis of the network of H-bonds with BF_4 as compared to the Br case, the interaction energy E_b with BF_4 is much larger than that with Br (Table 3). As a chelating anion and a good H-bond acceptor, acetate gives a large interaction energy for both isomers. These ion-pair formation energies are comparable to binding energies of a weak ligand like H_2 and should thus be considered more carefully in any theoretical reactivity study of organometallic salts.

Our results suggest that when several protons of similar acidity are close, a multidentate anion such as BF_4 will search for the most efficient network of interactions, whereas an anion like Br will prefer to create one strong interaction with the most acidic center. In any intramolecular proton transfer, the BF_4 anion would be expected to find it hard to "follow" the migrating proton, while at the same time trying to maintain its network of H-bonds. In contrast, if the transferring proton is the most acidic, then the Br anion would gain in "following" the transferring hydrogen at the expense of less acidic protons in an anion-coupled proton transfer. The difference in behavior will be fully expressed in the transition state for C−H activation, and the outcome will result from the competition between (i) maximum H-bonding stabilizing interaction versus (ii) minimal steric impact from the anion.

(2) Computational Studies of the Reaction Mechanism. The computational study of the reaction pathways leading to the normal and abnormal carbene was carried out on a model system consisting of $IrH_3(PMe_3)_2$ and the *N*,*N*′-dimethylimidazolium cation in the presence of A^- where A = BF_4 or Br. This modeling is considered appropriate because prior mechanistic work[36] shows that (i) the reactions of IrH_5L_2 proceed via initial H_2 loss and (ii) very similar results are found whether we use the chelate imidazolium salt or a mixture of *N*,*N*′-dialkyl imidazolium salt and free pyridine (eq 2).[42] The reaction is proposed to start by loss of H_2 to generate IrH_3L_2 followed by a C−H bond activation of the imidazolium salt with formation of an H_2 complex,[44] in turn followed by the replacement of the H_2 ligand by the pyridine (see Figure 3). The pathways corresponding to the activation of C2−H and C5−H are named N and AN, respectively. The activated C−H is named C−H_{ac}, and the uncleaved C−H bond is named C−H_{un}.

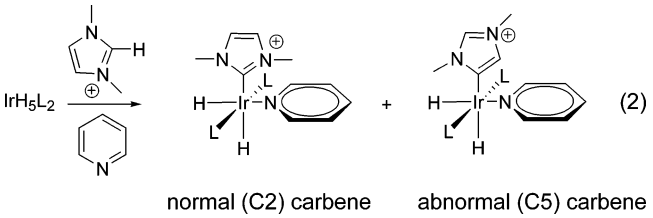

Anion-free reaction pathways were examined first, but, although the transition state for activation of C5−H was found, no transition state could be located for C2−H and therefore only reaction pathways in the presence of anion are discussed. The structures of all extrema are shown in Figure 4 for BF_4 and in Figure 5 for Br.

Reactions in the Presence of BF_4. $IrH_3(PMe_3)_2$ is a square-based pyramid with an apical hydride and a pair of mutually trans basal hydrides. The LUMO is the well-known d_{z^2}-based orbital (*z* apical). Interestingly, the HOMO is not a metal d orbital but the out-of-phase combination of the two basal hydrides. Thus, in addition to the usual Lewis acid property

(44) Kubas, G. J. *Metal Dihydrogen and σ−Bond Complexes: Structure, Theory and Reactivity*; Kluwer Academic Publishers: New York, 2001.

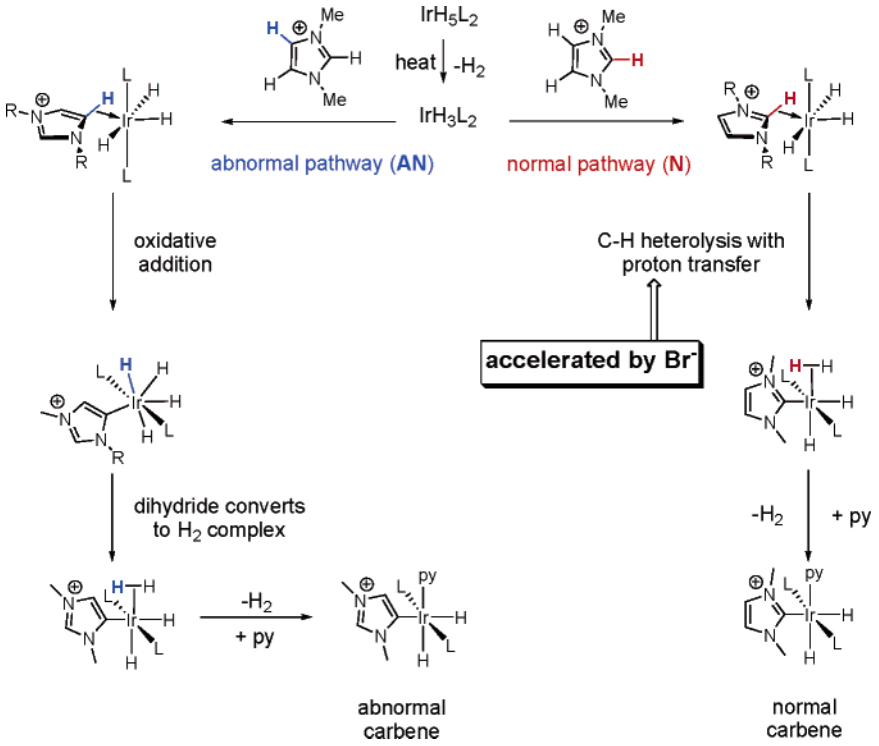

Figure 3. The proposed normal (N) and abnormal (AN) pathways (L = PMe_3).

associated with the LUMO, the metal fragment has some Lewis base activity associated with the basal hydrides.

The reaction starts with formation of a σ-complex of the C−H bond to be cleaved, C−H_{ac}, which binds trans to the apical hydride. In both the AN and the N paths, the coordinated C−H bond is oriented perpendicular to the IrH_3 plane and the imidazolium ring plane is perpendicular to the IrL_2(C−H_{ac}) plane. The metric data for the σ-complex differ slightly for the two cases (Ir−C = 2.334 Å, Ir···H_{ac} = 1.821 Å for AN; Ir−C = 2.360 Å, Ir···H_{ac} = 1.900 Å for N). The BF_4 anion is located above the imidazolium ring with one F_a pointing toward C−H_{ac}, and another, F_b, toward the other C−H bond, C−H_{un} (both shown with dotted lines in Figure 4). The BF_4 is much closer to the azolium ring in the AN pathway: the F_a···H_{ac} distance being 2.306 Å for AN but 3.895 Å for N. The anion therefore interacts more strongly with H_{ac}, and the distance is even shorter when C−H_{ac} is C2−H (N path). Any H···F distance longer than 2.3 Å can be considered a weak interaction, as is the case for all except the C2−H_{ac}/BF_4 combination. In all cases, a large number of weak interactions are also present involving the IrH_3-$(PMe_3)_2$, the imidazolium ion, and the BF_4; in particular, the acidic *N*-methyl groups are close to the basic basal hydrides and the BF_4 is not far from two methyl groups of the PMe_3 ligand. The details of these interactions will no doubt be different in the real experimental systems, which contain PPh_3 and not PMe_3, but in what follows, we will concentrate on the main interactions that do not involve PR_3 and are expected to be common for both.

The metal remains octahedral in the transition state, the NHC carbon being one of the ligands. The imidazolium rotates from the position it had in the σ-complex, so as to bring the C−H proton closer to the hydride to which proton transfer is to occur, and the NHC ligand follows this motion so that it is no longer perpendicular to the plane containing the phosphine ligands. The C−H bond cleavage is more advanced in the N pathway (C2−H = 1.429 Å) than in the AN path (C5−H = 1.384 Å), and the Ir−C bond is accordingly shorter in the N case (Ir−C2 = 2.157 Å) than in the AN case (Ir−C5 = 2.188 Å). The interaction between BF_4 and the imidazolium ring is based on principles similar to those in the reactants: F_a is close to H_{ac} and F_b is close to H_{un}. The F···H distance is the shortest for C2−H_{ac} (N path), where the F_a···H_{ac}−C2 is 1.984 Å but F_b···H_{un}−C5 is 3.114 Å. In the AN case, the F_a···H_{ac}−C5 distance is 2.40 Å, and F_b is only 2.789 Å from H−C2.

In the AN case, the transition state leads to a pentagonal bipyramidal Ir^V intermediate with four equatorial H ligands and an equatorial carbene. The Ir−C5 distance of 2.128 Å indicates a single Ir−C bond. The BF_4 lies above the imidazolium ring, near the C−H_{un}, with H_{un}···F_b being 2.130 Å. In an important difference between the two paths, the N path transition state leads not to an Ir^V species but to an Ir^{III} dihydrogen complex with H_2 trans to hydride and cis to the NHC. The H_2 ligand and the NHC are twisted relative to the IrH_3 plane. The BF_4 is close to the protonic dihydrogen ligand with an H···F_a distance of 2.036 Å.

Reactions in the Presence of Br. The nonchelating Br anion cannot optimally simultaneously interact with two different H atoms of the imidazolium group but prefers to interact strongly with one H, the choice being either H_{ac} or H_{un}. The basic features of the minima and transition states are similar for the two anions. The reactant is a σ-complex with the C−H bond in the plane perpendicular to the IrH_3 plane. For the AN path, Br is far from H_{ac} but close to H_{un} (Br···H_{un} = 2.766 Å). For the N path, Br is close to H_{ac} with the angle Cl···H_{ac}···Ir being 158°. At the transition state for the AN path, Br is close to H_{un} (2.876 Å) and far from H_{ac} (>4 Å). In contrast, for the N path, Br is very close to H_{ac} (H_{ac}···Br = 2.403 Å) with a Br−H_{ac}−Ir angle of 164.9°. In the tetrahydride intermediate formed from the AN

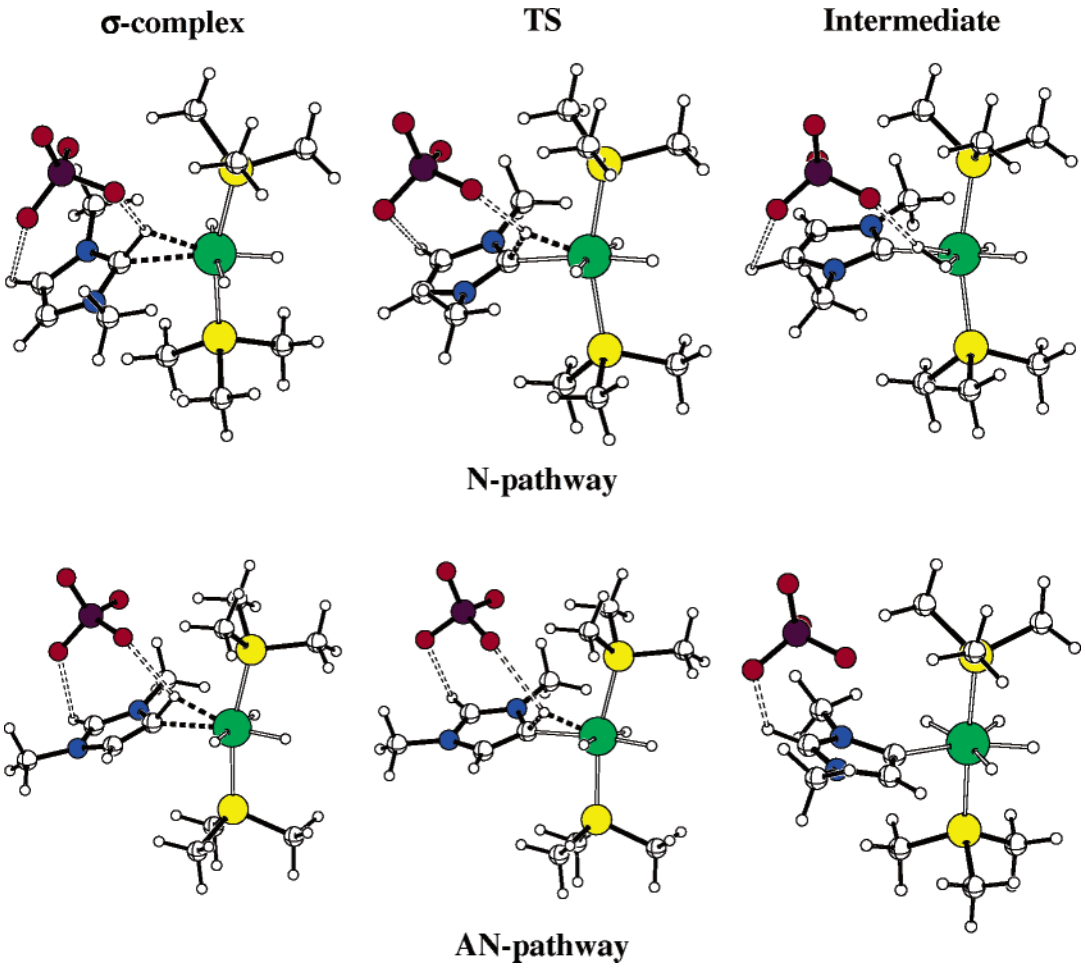

Figure 4. Optimized geometries for the σ-complex, transition state, and intermediate located along the N and AN pathways with BF_4 as counteranion. In an important difference between the two pathways, the N intermediate is an Ir^{III} complex of H_2 and the AN intermediate is an Ir^{V} polyhydride. Energy profiles (kcal mol^{-1}) relative to the σ-complex: N pathway, 2.6 (TS), −17.5 (intermediate); AN pathway, 2.0 (TS), −19.9 (intermediate).

transition state, the Br anion is near H_{un} ($Br\cdots H_{un}$ = 3.00 Å). In the dihydrogen complex formed from the N transition state, the Br anion is very close to the dihydrogen ligand (shortest $Br\cdots H$ distance = 2.528 Å). These geometrical features for the minima and transition state (extrema) on the two paths show that the Br always prefers to be near H−C2 rather than H−C5, and this preference is enhanced when H−C2 is the bond being activated.

Energy Profiles for C−H Bond Activation and Discussion. After initial H_2 loss, the reaction continues with the coordination of the imidazolium/anion ion-pair to $IrH_3(PMe_3)_2$ via a C−H σ-complex. Although the resulting pair of σ complexes could be calculated for coordination at C2−H (N) and at C5−H (AN), the relative free energies of these two species versus the separated imidazolium/anion and $IrH_3(PMe_3)_2$ fragment are not easy to evaluate. The anion is paired with the more acidic C2−H in the imidazolium/anion ion-pair in a C−H···A hydrogen bond. Coordination to C5−H thus does not require much structural reorganization because this bond is remote from the anion. This is not the case for coordination at C2−H where the anion has to be displaced. These changes, which of course occur in a polar solvent, cannot be easily evaluated with the present level of theory. Therefore, the relative population of the two σ-complexes cannot be evaluated and is certainly not well represented by the calculated difference in electronic energies between the two systems (6 kcal mol^{-1} in favor of the σ-complex at H−C2 in the gas phase and 2 kcal mol^{-1} in the THF solvent with BF_4 as the counteranion). In the absence of better information, we have analyzed the computational profiles by focusing on the energy barriers $\Delta E^{\ddagger}$ from each of the σ-complexes (Table 4). The activation energies $\Delta G^{\ddagger}$, also given in Table 4, show similar trends, and so we have chosen to discuss the results based on $\Delta E^{\ddagger}$.

The fact that we could not locate a transition state for activation of the C2−H bond in absence of counteranion is in line with a previous finding that the activation of the C2−H bond of an imidazolium salt, in the absence of the counteranion, by a Pd(0) diphosphine species occurs without any energy barrier.[24a] The energy barrier found in the present study for the activation of the C5−H was 0.2 kcal mol^{-1}. In the presence of anions, both energy barriers are nonzero but very small. After passage of the transition state, the energy profile goes sharply downward. In the case of Br, the energy barrier for the AN path is 3.8 kcal mol^{-1} and only 2.5 kcal mol^{-1} for the N path. With BF_4, the respective values are 2.0 and 2.6 kcal mol^{-1} (Me/Me entries in Table 4). These results show that there is no great kinetic preference for activating either the C2−H or the C5−H bonds despite the fact that in many decades of work on the metalation of imidazolium salts up to 2002, only the normal C2 NHC products were ever observed, presumably because NHCs were only very rarely synthesized by C−H bond activation. The results also suggest that the nature of the anion

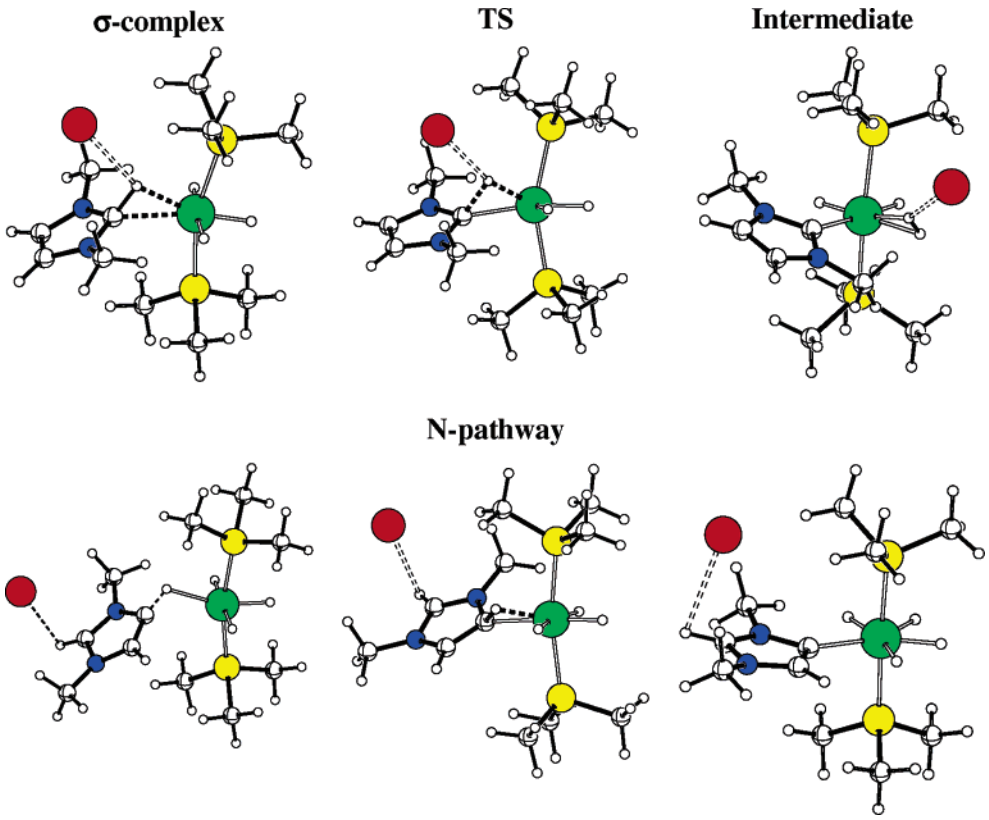

Figure 5. Optimized geometries for the σ-complex, transition state, and intermediate located along the N and AN pathways with Br as counteranion. The intermediates are Ir^{III} (N) and Ir^{V} (AN) as in the BF_4 pathway of Figure 4. Energy profiles (kcal mol^{-1}) relative to the σ-complex: N pathway, 2.5 (TS), −18.6 (intermediate); AN pathway, 3.8 (TS), −16.5 (intermediate).

Table 4. Energetics (kcal mol^{-1}) Associated with the N and AN Pathways Calculated for *N*,*N*′-Dialkyl-imidazolium Salts of BF_4 or Br Reacting with $IrH_3(PMe_3)_2$[a]

anion	subst.	path	$\Delta E^{\ddagger}$	ΔE	$\Delta G^{\ddagger}$	ΔG
BF_4	Me/Me	N	2.6	−17.5	1.9	−17.0
		AN	2.0	−19.9	1.5	−20.3
BF_4	Me/^{i}Pr	N	2.3	−16.7	1.7	−16.0
		AN	2.7	−18.3	3.1	−16.4
BF_4	^{i}Pr/Me	N	4.2	−11.9	3.3	−10.3
Br	Me/Me	N	2.5	−18.6	0.3	−19.3
		AN	3.8	−16.5	3.2	−16.1
Br	Me/^{i}Pr	N	2.5	−18.5	0.8	−17.8
		AN	3.5	−16.4	3.6	−16.5

[a] The notation R/R′ (R = Me, ^{i}Pr; R′ = Me, ^{i}Pr) indicates a C−H oxidative process where the migrating proton is adjacent to the R group (see Scheme 1). The activation barriers ($\Delta E^{\ddagger}$ and $\Delta G^{\ddagger}$) and reaction energies (ΔE and ΔG) are evaluated from the corresponding σ-complex in each case. N (respectively AN) refers to the N (respectively AN) pathway.

Scheme 1. The Two Possible Trajectories from the σ-Complex at C2−H of the *N*-Methyl-*N*′-isopropyl Imidazolium Cation with IrH_3L_2 (L = PMe_3)

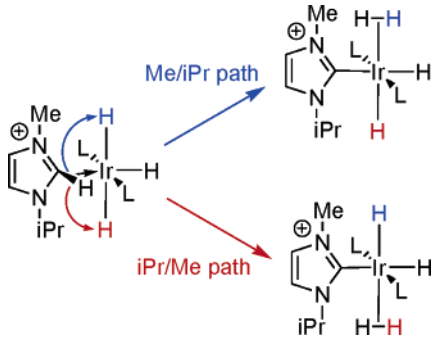

tunes the outcome in a subtle way. One can hardly consider differences in barrier height of less than 1 kcal mol^{-1} as reliable. Nevertheless, the lower barrier calculated for the N path in the case of Br is consistent with the formation of the normal NHC with Br, and the lower barrier for the AN path in the case of BF_4 is consistent with the formation of the abnormal NHC with BF_4.

To understand the substituents effects, the same calculations were carried out on the *N*-methyl-*N*′-isopropyl imidazolium salt. Even though the starting σ-complex in the calculations for the normal pathway had a geometry such that the proton could migrate to either of the pair of trans hydrides (Scheme 1), when an ^{i}Pr group is present, the symmetry is broken, and in one trajectory, the proton needs to pass by the ^{i}Pr group (^{i}Pr/Me in Table 4), and in the other, the Me group (Me/^{i}Pr in Table 4). For BF_4, the more hindered trajectory is calculated to have a significantly higher barrier (^{i}Pr/Me, 4.2 kcal mol^{-1}; Me/^{i}Pr, 2.3 kcal mol^{-1}). For the Br anion, the Me/^{i}Pr trajectory is the only one obtained and has an activation barrier similar to the Me/Me case (2.5 kcal mol^{-1}). All attempts to find a TS for the ^{i}Pr/Me trajectory with Br failed as rotation of the imidazolium in the optimization procedure switched the pathway to the less hindered Me/^{i}Pr trajectory. Unlike the BF_4 anion, the bromide needs to track the proton and cannot do so efficiently if it has to approach a bulky group.

For the AN reaction, the calculations were carried out with the C−H_{ac} bond next to the methyl group (Me/^{i}Pr in Table 4, A = BF_4, Br) as this is the major regioisomer observed in the experiment.[42] In the σ-complex, the change of methyl to isopropyl shifts the anion away from the imidazolium ring to

minimize repulsion with the *i*-Pr group. Because BF_4 cannot easily interact with the distant azole C−H_{ac} bonds, it compensates by moving close to C−H_{un}. Remarkably, this significantly lengthens the Ir−C bond (2.334 Å, Me/Me; 2.517 Å, Me/^{i}Pr). In the AN transition state for C−H activation, the BF_4 remains quite far from the C−H_{ac} bond and close to H−C2. This contrasts with the *N*,*N*′-dimethyl-imidazolium case where the BF_4 approaches the C5−H being cleaved. This shows that although BF_4, as a chelating anion, is able to interact with two H atoms of the imidazolium, it does so preferentially with H−C2, especially when it is the C−H bond being cleaved, and does not approach H−C5 even if cleaved, plausibly because of the steric effect of the isopropyl group.

The calculations show that the barriers are similar for the *N*,*N*′-dimethyl-imidazolium and *N*-methyl-*N*′-isopropyl-imidazolium salts in the case of Br, because the proton prefers to pass by the methyl group and, therefore, never approaches the more bulky ^{i}Pr substituent. However, the preference for activation of C5−H over C2−H is increased with BF_4 in the *N*-methyl-*N*′-isopropyl case: BF_4 is prevented from approaching the more acidic H−C2 by the bulky isopropyl ligand in the N path, whereas it can approach it while staying far from the isopropyl group in the AN path. These results are consistent with the experimental data: the AN/N ratio is larger for the *N*-methyl-*N*′-isopropyl imidazolium/BF_4 salt than for the *N*,*N*′-dimethyl case (Table 1). Although this should be considered as a fortuitous agreement, the discussion below suggests that a deeper analysis of the calculations does allow us to identify the essential features of the anion effect.

The C−H activation step has an exothermicity of between 16 and 20 kcal mol^{-1}, consistent with the experimental absence of a back reaction that would allow isomerization of AN to N product. This result also agrees with the computational studies of Cavell *et al*.[24a] The formation of a tetrahydride NHC intermediate for the AN path and a dihydrogen−NHC complex for the N path in the present study is readily rationalized on the basis that the stronger donor power of the abnormal NHC favors Ir^V over Ir^{III}.[42] The displacement of the labile H_2 ligand by pyridine can readily occur for the dihydrogen intermediate on the N path but requires another step for the tetrahydride in the AN path. The transition state for the formation of the dihydrogen−NHC complex from the tetrahydride was located for the case of BF_4. The energy barrier from the tetrahydride complex is only 2.1 kcal mol^{-1}, and the dihydrogen complex lies 0.9 kcal mol^{-1} above the tetrahydride complex. In this dihydrogen complex, BF_4 remains near the unactivated H−C2 bond. The transformation of the tetrahydride into the dihydrogen complex is thus facile, and the replacement of the dihydrogen by pyridine leading to the final NHC-pyridine complex is thus facile for both N and AN pathways.

The role of the anion in the various extrema can be rationalized from the NBO charges and Wiberg bond indices (see Table S2 in the Supporting Information). The azole−BF_4 interaction is spread over several H centers and several F atoms for the two pathways according to the geometric constraints. Consequently, no one F has any very strong interaction with any one H as suggested by the Wiberg indices. The activation of the imidazolium C−H bond by the metal−hydride fragment can occur via a redox or a heterolytic process with proton transfer from the imidazolium to the hydride ligand. Because of the geometrical constraints that impose a substantial distance between the carbon of the NHC and the *cis* hydride, a counteranion is necessary to stabilize the migrating proton in the transition state in an anion-coupled proton transfer. Br is a much more effective anion for this purpose than BF_4. Although the BF_4 is not far from the C−H_{ac} hydrogen in the N transition state, it is not very effective in stabilizing this transition state because of the delocalization of the negative anionic charge over the four fluorine atoms. Thus, the preferred transition state for BF_4 is an oxidative addition of the only moderately polar C5−H bond, where the BF_4 anion stabilizes the unactivated but more acidic C2−H bond. In contrast, the ion-pairing interaction with the nonchelating, small Br essentially involves only one imidazolium H. Bromide is therefore able to approach close to, and to strongly stabilize, a transferring proton; this favors the heterolytic cleavage, which is also preferred for the more acidic C2−H bond.

In the critical finding of this study, the significantly larger H_{ac}···Br Wiberg bond index (0.120) at the transition state for the N pathway versus that in the σ-complex (0.049) suggests that H_{ac} has become more protonic to interact with Br. None of the other pathways presents the same features (Table S2 in the Supporting Information). Thus, in the presence of the Br anion, the activation of C2−H is a proton transfer from the imidazolium cation to the hydride on the metal. This nonredox process naturally leads to the formation of an Ir^{III}−dihydrogen complex as the intermediate formed immediately after the C−H bond activation.

Conclusion

Changing counteranion in 2-pyridylmethyl imidazolium salts along the series Br, BF_4, PF_6, SbF_6 causes their kinetic reaction products with $IrH_5(PPh_3)_2$ to be switched from chelating NHCs having normal C2 to ones having abnormal C5 binding. Ion pairing is detected in the products by NMR studies. Both computational and NMR studies suggest that the anions are bound near the NHC group. In the abnormal NHC, the C−H bond at C2 that points away from the metal becomes the site of ion-pairing. This C−H bond is highly acidic so the ion-pairing in a C−H···A hydrogen bond (A = anion) is particularly strong for the abnormal NHC. The computational study suggests that the relative energetics of the normal versus the abnormal forms is strongly affected by choice of anion, hence the big anion effects observed. Despite the abnormal free carbene being nearly 15 kcal mol^{-1} less stable than the normal one, the two forms become close to isoenergetic on metal binding and ion-pair formation because of the strong ion-pairing to the abnormal NHC.

The apparent complexity of the system in fact reduces to a few simple points as a result of the computational work. For a significant anion effect on the regioselectivity, the two competing paths have to have similar barriers but go by different mechanisms. For a significant selectivity change, the two transition states must be differentially stabilized by the anion, relative to their respective ground states, so that the relative barrier heights show an anion dependence. In the present case, the AN path involving oxidative addition is expected to show little anion dependence, because there are no great changes in the charge distributions during the reaction. The heterolytic N path, with its strongly protonic H migration, shows a particularly

strong H···Br interaction, as judged by the Wiberg index in the transition state, leading to a big acceleration by Br. The small Br anion can readily accommodate itself to the proton motion from the imidazolium C−H to the adjacent Ir−H in what can be termed an anion-coupled proton transfer.

The reason for the change of mechanism is the very strong donor character of the abnormal NHC, which favors attainment of Ir^V in the AN path versus the highly protonic character of the C2−H of an imidazolium salt that favors the heterolytic C−H activation of the N path. This relatively rare case of an anion-dependent selectivity change is therefore explained by a relatively rare coincidence of several criteria. A search for further examples would help confirm or deny the general principles proposed here.

The results emphasize a potentially important caveat for workers in the field not to assume that the choice of counterion is immaterial for organometallic reactivity. They could also offer a potentially important opportunity in that change of anion may be a more generally useful method of tuning selectivity, than currently believed, especially in asymmetric catalysis where the two pathways necessarily have similar barriers.

Experimental Section

All operations were carried out under argon atmosphere using standard Schlenk techniques. Solvents were dried over calcium hydride (CH_2Cl_2) or sodium/benzophenone (Et_2O). Solvents were degassed prior to use. IR spectra were recorded on a Midac M1200 FT-IR spectrometer. Microanalyses were carried out by Robertson Microlit Laboratories and Atlantic Microlabs, Inc., and the presence of the appropriate solvents of crystallization was verified by proton NMR. NMR spectra were either recorded on GE Omega 300, GE Omega 500, Bruker 400, or Bruker 500 MHz spectrometers, and chemical shifts were measured by reference to the residual solvent resonance or by reference to external TMS (^{1}H and ^{13}C), $CFCl_3$ (^{19}F), and 85% H_3PO_4 (^{31}P).

$IrH_5(PPh_3)_2$,[45] *N*-methyl-*N*′-(2-pyridylmethyl)imidazolium bromide (**2**),[46] and $[H_2Ir(OCMe_2)(PPh_3)_2]$ BF_4[47] were prepared according to literature methods; all other reagents that are commercially available were used as received. Assignments are based on COSY and HMQC spectroscopy.

NOE NMR Measurements. The ^{1}H-NOESY NMR experiments[48] were acquired by the standard three-pulse sequence or by the PFG version.[49] Two-dimensional ^{19}F,^{1}H-HOESY NMR experiments were acquired using the standard four-pulse sequence or the modified version.[50] The number of transients and the number of data points were chosen according to the sample concentration and to the desired final digital resolution. Semiquantitative spectra were acquired using a 1 s relaxation delay and 800 ms mixing times.

PGSE NMR Measurements. ^{1}H and ^{19}F PGSE NMR measurements were performed by using the standard stimulated echo pulse sequence[40a] on a Bruker AVANCE DRX 400 spectrometer equipped with a GREAT 1/10 gradient unit and a QNP probe with a Z-gradient coil, at 296 K without spinning. The shape of the gradients was rectangular, their duration (δ) was 4−5 ms, and their strength (G) was varied during the experiments. All of the spectra were acquired using 32K points, a spectral width of 5000 (^{1}H) and 18 000 (^{19}F) Hz, and processed with a line broadening of 1.0 (^{1}H) and 1.5 (^{19}F) Hz. The semilogarithmic plots of $\ln(I/I_0)$ versus G^2 were fitted using a standard linear regression algorithm; the R factor was always higher than 0.99. Different values of Δ, "nt" (number of transients), and number of different gradient strengths (G) were used for different samples. The methodology for treating the data was described previously.[51]

***N*-Isopropyl-*N*′-(2-pyridylmethyl)imidazolium Bromide (1h).** 2-Bromomethylpyridine hydrobromide (Aldrich, 1.01 g, 4.0 mmol) was neutralized using saturated aqueous sodium carbonate. The liberated 2-bromomethylpyridine was extracted into diethyl ether (3 × 30 mL) at 0 °C, dried with magnesium sulfate, and added to a solution of 1-isopropylimidazole (0.44 g, 4.0 mmol) in 1,4-dioxane (30 mL). The ether was removed under reduced pressure, and the solution was refluxed for 12 h. The volatiles were removed in vacuo, and the oil so formed was purified by repetitive precipitation from MeOH/Et_2O and finally recrystallized from CH_2Cl_2/Et_2O to give colorless crystals Yield: 0.68 g (60%). ^{1}H NMR ($CHCl_3$, 298 K): δ 10.97 (s, 1H, NCHN), 8.56−8.52 (m, 1H, H_{py}), 7.93 (d, 1H, $^3J_{HH}$ = 7.8 Hz, H_{py}), 7.75 (dt, 1H, $^4J_{HH}$ = 1.7 Hz, $^3J_{HH}$ = 7.5 Hz, H_{py}), 7.65 (t, 1H, $^3J_{HH}$ = 1.5 Hz, H_{im}), 7.31−7.24 (m, 1H, H_{py}), 7.22 (t, 1H, $^3J_{HH}$ = 1.5 Hz, H_{im}), 5.81 (s, 4H, CH_2), 4.74 (septet, 1H, $^3J_{HH}$ = 6.7 Hz, CH), 1.63 (d, 6H, $^3J_{HH}$ = 6.7 Hz, CH_3). ^{13}C{^{1}H} NMR ($CDCl_3$, 298 K): δ 152.57 (C_{py}), 149.72 (C_{py}), 137.80 (C_{py}), 136.80 (NCN), 124.60 (C_{py}), 124.06 (C_{py}), 122.78 (C_{im}), 118.65 (C_{im}), 53.86 (CH_2), 53.43 (CH), 23.09 (2C, CH_3); mp = 85−86 °C. Anal. Calcd for $C_{12}H_{16}BrN_3 \cdot H_2O$ (282.18): C, 48.01; H, 6.04; N, 14.00. Found: C, 48.33; H, 5.81; N, 14.10.

***N*-Butyl-*N*′-(2-pyridylmethyl)imidazolium Bromide (1j).** In a modification of the procedure of Danopoulos et al.,[52] 2-(bromomethyl)-pyridine hydrobromide (4.0 g, 16 mmol) was neutralized using a saturated aqueous sodium carbonate. The liberated 2-bromomethylpyridine was extracted into diethyl ether (3 × 30 mL) at 0 °C, dried with magnesium sulfate, and filtered. 1-Butylimidazole (1.95 g, 16.0 mmol) in methanol (100 mL) was added at 0 °C, the ether was removed under reduced pressure, and the solution was stirred at room temperature for 12 h. The methanol was then evaporated under reduced pressure, and the oil so formed was purified by repeated precipitation from CH_2Cl_2/Et_2O. The resulting oily product was dried in vacuo. Yield: 4.52 g (95%). ^{1}H NMR ($CHCl_3$, 298 K): δ 10.44 (s, 1H, NCHN), 8.49 (d, 1H, $^3J_{HH}$ = 5.0 Hz, H_{py}), 7.80 (d, 1H, $^3J_{HH}$ = 7.7 Hz, H_{py}), 7.74−7.69 (m, 1H, H_{py}), 7.67 (s, 1H, H_{im}), 7.42 (s, 1H, H_{im}), 7.28−7.24 (m, 1H, H_{py}), 5.77 (s, 2H, CH_2), 4.27 (t, 2H, $^3J_{HH}$ = 7.5 Hz, CH_2), 1.91−1.82 (m, 2H, CH_2), 1.39−1.29 (m, 2H, CH_2), 0.91 (t, 2H, $^3J_{HH}$ = 7.5 Hz, CH_3). ^{13}C{^{1}H} NMR ($CDCl_3$, 298 K): δ 152.32 (C_{py}), 149.52 (C_{py}), 137.80 (C_{py}), 136.98 (NCN), 124.08 (C_{py}), 123.99 (C_{py}), 122.80 (C_{im}), 121.56 (C_{im}), 53.61 (CH_2), 49.86 (CH_2), 31.92 (CH_2), 19.36 (CH_2), 13.33 (CH_3). Anal. Calcd for $C_{13}H_{18}BrN_3 \cdot 1.5H_2O$: C, 48.31; H, 6.55; N, 13.00. Found: C, 47.85; H, 6.54; N, 12.96.

(η^2-C,N)(*N*-Methyl-*N*′-(2-pyridylmethyl)imidazole-2-ylidene)bis-(hydrido)bis(triphenylphosphine)iridium(III) Bromide (2a). *N*-Methyl-*N*′-(2-pyridylmethyl)imidazolium bromide (36 mg, 0.14 mmol) and $IrH_5(PPh_3)_2$ (100 mg, 0.140 mmol) in THF (18 mL) were vigorously refluxed in air for 2 h. After the mixture was cooled to room temperature, about 10 mL of THF was removed in vacuo, and 60 mL of pentane was added. A white precipitate was filtered off and dried in vacuo. Yield: 95 mg (70%). Pure **2a** can be obtained by recrystallization from $CHCl_3$/pentane.

^{1}H NMR ($CDCl_3$, 298 K): δ 8.04 (d, 1H, $^3J_{HH}$ = 7.5 Hz, H_{py}), 7.98 (d, 1H, $^3J_{HH}$ = 5.5 Hz, H_{py}), 7.96 (d, 1H, $^3J_{HH}$ = 1.5 Hz, H_{im}), 7.51 (t, 1H, $^3J_{HH}$ = 7.0 Hz, H_{py}), 7.34−7.18 (m, 30H, H_{ph}), 6.31 (d, 1H, $^3J_{HH}$ = 1.6 Hz, H_{im}), 6.14 (t, 1H, $^3J_{HH}$ = 6.7 Hz, H_{py}), 5.33 (s, 2H, CH_2), 2.51 (s, 3H, CH_3), −11.17 (dt, $^3J_{HH}$ = 5.1 Hz, $^2J_{PH}$ = 19.8 Hz, Ir−H), −21.00 (dt, $^3J_{HH}$ = 5.0 Hz, $^2J_{PH}$ = 17.2 Hz, Ir−H). ^{13}C{^{1}H} NMR ($CDCl_3$, 298 K): δ 169.78 (t, J_{PC} = 6.7 Hz, $C_{carbene}$), 160.61 (C_{py}), 153.06 (C_{opy}), 137.70 (C_{opy}), 134.11 (t, J_{PC} = 26.9 Hz, C_{ph}), 133.24 (t,

(45) Crabtree, R. H.; Felkin, H.; Morris, G. E. *J. Organomet. Chem.* **1977**, *141*, 205.
(46) McGuiness, D. S.; Cavell, K. J. *Organometallics* **2000**, *19*, 741.
(47) Crabtree, R. H.; Demou, P. C.; Eden, D.; Mihelcic, J. M.; Parnell, C. A.; Quirk, J. M.; Morris, G. E. *J. Am. Chem. Soc.* **1982**, *104*, 6994.
(48) Jeener, J.; Meier, B. H.; Bachmann, P.; Ernst, R. R. *J. Chem. Phys.* **1979**, *71*, 4546.
(49) Wagner, R.; Berger, S. *J. Magn. Reson., Ser. A* **1996**, *123*, 119.
(50) Lix, B.; Sönnichsen, F. D.; Sykes, B. D. *J. Magn. Reson., Ser. A* **1996**, *121*, 83.
(51) Zuccaccia, D.; Macchioni, A. *Organometallics* **2005**, *24*, 3476.
(52) Tulloch, A. A. D.; Danopoulos, A. A.; Winston, S.; Kleinhenz, S.; Eastham, G. *J. Chem. Soc., Dalton Trans.* **2000**, 4499.

J_{PC} = 6.0 Hz, C_{ph}), 129.99 (C_{ph}), 128.11 (t, J_{PC} = 4.8 Hz, C_{ph}), 126.66 (C_{py}), 123.54 (C_{py}), 123.41 (C_{im}), 120.32 (C_{im}), 54.75 (CH_2), 37.08 (CH_3). $^{31}P\{^1H\}$ NMR ($CDCl_3$, 298 K): δ 19.05. Anal. Calcd for $C_{46}H_{43}BrIrN_3P_2.2CHCl_3$: C, 47.62; H, 3.75; N, 3.47. Found: C, 47.95; H, 3.73; N, 3.47.

Ion Exchange of Bromide for Tetrafluoroborate. The imidazolium bromide salt is dissolved in a small quantity of dichloromethane and loaded onto a silica gel column (prepared with ethyl acetate). Sufficient ethyl acetate is run through the column to remove any mobile materials (200−300 mL). The salt is eluted with a solution of 2 equiv of $NaBF_4$ in 500 mL of acetone. In some cases, further elution with pure acetone was required to complete the elution. Using additional $NaBF_4$ results in contamination. After collection of the eluate fractions, and removal of the acetone by rotary evaporator, the residue is dissolved in a large quantity of dichloromethane, filtered through Celite to remove any excess $NaBF_4$, and the solvent is then evaporated to yield a brown-yellow oil (R = ^{n}Bu) or yellow crystals (R = ^{i}Pr) of the BF_4^- salt. Yields vary between 65% and 75%.

(η^2-C,N)(*N*-Isopropyl-*N*′-(2-pyridylmethyl)imidazole-2-ylidene)-dihydridobis(triphenylphosphine)iridium(III) Tetrafluoroborate (2i). $[H_2Ir(OCMe_2)_2(PPh_3)_2]BF_4$ (178 mg, 0.194 mmol) and *N*-isopropyl-*N*′-(2-pyridylmethyl)imidazolium tetrafluoroborate (**1i**) (56 mg, 0.19 mmol) were combined in dichloromethane (12 mL) and stirred at room temperature for 1 h. Excess sodium bicarbonate was then added, and the mixture was stirred for 30 min, during which time the color changed from red-orange to gray-green. The solution was then filtered through Celite, and the solvent was removed by rotary evaporation. The crude product was dissolved in ca. 2 mL of dichloromethane and layered with pentane. After standing overnight, the mixture separated into a dark oil and a clear supernatant that was separated, the solvent was removed in vacuo, and the resulting white powder was recrystallized from dichloromethane/pentane to yield translucent crystals of the product. Yield: 54 mg (28%).

^1H NMR (CD_2Cl_2 δ 5.32, 298 K): δ 7.85 (d (broad), 1H, $^3J_{HH}$ = 5.7 Hz, H_{py}), 7.55 (td, 1H, $^3J_{HH}$ = 7.7 Hz, $^4J_{HH}$ = 1.4 Hz, H_{py}), 7.33 (m, 8H, H_{Ph}), 7.24 (m, 12H, H_{Ph}, H_{im}), 7.19 (m, 12H, H_{Ph}, H_{py}), 6.72 (d, 1H, $^3J_{HH}$ = 2.0 Hz, H_{im}), 6.28 (ddd, 1H, $^3J_{HH}$ = 7.4 Hz $^4J_{HH}$ = 5.7 Hz, $^5J_{HH}$ = 1.4 Hz, H_{py}), 4.72 (s, 2H, CH_2), 4.12 (sept, 1H, $^3J_{HH}$ = 6.8 Hz, NC*H*(CH_3)$_2$), 0.465 (d, 6H, $^3J_{HH}$ = 6.8 Hz, NCH(C*H*$_3$)$_2$), −11.27 (td, 1H, $^2J_{PH}$ = 21.2 Hz, $^2J_{HH}$ = 5.1 Hz, Ir−H), −20.92 (td, 1H, $^2J_{PH}$ = 16.9 Hz, $^2J_{HH}$ = 5.1 Hz, Ir−H). $^{13}C\{^1H\}$ NMR (CD_2Cl_2 δ 54.0, 298 K): δ 169.79 (t, $^2J_{PH}$ = 7.1 Hz, $C_{carbene}$), 161.22 (C_{py}), 154.03 (C_{py}), 138.63 (C_{py}), 134.81 (t, J_{PC} = 26.4 Hz, C_{Ph}), 134.04 (t, J_{PC} = 5.8 Hz, C_{Ph}), 130.80 (C_{Ph}), 128.84 (t, J_{PC} = 4.9 Hz, C_{Ph}), 125.75 (C_{py}), 124.69 (C_{py}), 122.88 (C_{im}), 117.46 (C_{im}), 56.40 (CH_2), 52.51 (*C*H(Me)$_2$), 21.90 (CH(*C*H$_3$)$_2$). $^{31}P\{^1H\}$ NMR (CD_2Cl_2, 298 K): δ 17.21. Anal. Calcd for $C_{48}H_{47}BF_4IrN_3P_2$·THF: C, 57.88; N, 3.89; H, 5.14. Found: C, 57.68; N, 3.82; H, 5.13.

(η^2-C,N)(*N*-(*n*-Butyl)-*N*′-(2-pyridylmethyl)imidazole-2-ylidene)-dihydridobis(triphenylphosphine)iridium(III) Tetrafluoroborate (2j). $[H_2Ir(OCMe_2)_2(PPh_3)_2]BF_4$ (155 mg, 0.169 mmol) and *N*-(*n*-butyl)-*N*′-(2-pyridylmethyl)imidazolium tetrafluoroborate (**1j**) (51 mg, 0.17 mmol) were combined in dichloromethane and treated exactly as was the ^{i}Pr derivative above. Yield: 98 mg (55%).

^1H NMR (CD_2Cl_2 δ 5.32, 298 K): δ 8.00 (d, 1H, J_{HH} = 5.6 Hz, H_{py}), 7.60 (td, 1H, J_{HH} = 7.7 Hz, J_{HH} = 1.2 Hz, H_{py}), 7.42 (t, 1H, J_{HH} = 7.1 Hz, H_{py}), 7.38−7.20 (m, 31H, H_{Ph}, H_{im}), 6.51 (d, 1H, $^3J_{HH}$ = 1.8 Hz, H_{im}), 6.30 (ddd, 1H, J_{HH} = 7.1 Hz, J_{HH} = 5.6 Hz, J_{HH} = 1.2 Hz, H_{py}), 4.69 (s, 2H NC*H*$_2$Py), 2.96 (dd, 2H, $^3J_{HH}$ = 8.2 Hz, $^4J_{HH}$ = 7.2 Hz, NC*H*$_2$CH$_2$CH$_2$CH$_3$), 1.02−0.86 (m, 4H, NCH$_2$C*H*$_2$C*H*$_2$CH$_3$), 0.648 (t, 3H, $^3J_{HH}$ = 7.2 Hz, NCH$_2$C*H*$_2$CH$_2$C*H*$_3$), −11.11 (td, 1H, $^2J_{PH}$ = 20.4 Hz, $^2J_{HH}$ = 5.2 Hz, Ir−H), −20.93 (td, 1H, $^2J_{PH}$ = 20.4 Hz, $^2J_{HH}$ = 5.2 Hz, Ir−H). $^{13}C\{^1H\}$ NMR (CD_2Cl_2 δ 54.0, 298 K): δ 170.30 (t, $^2J_{PH}$ = 6.9 Hz, $C_{carbene}$), 161.52 (C_{py}), 153.90 (C_{py}), 138.62 (C_{py}), 134.64 (t, J_{PC} = 26.8 Hz, C_{Ph}), 133.89 (t, J_{PC} = 5.9 Hz, C_{Ph}), 130.66 (C_{Ph}), 128.72 (t, J_{PC} = 4.6 Hz, C_{Ph}), 125.84 (C_{py}), 124.63 (C_{py}), 122.55 (C_{im}), 120.50 (C_{im}), 56.13 (N*C*H$_2$Py), 50.88 (N*C*H$_2$CH$_2$CH$_2$CH$_3$), 31.54 (NCH$_2$*C*H$_2$CH$_2$CH$_3$), 20.34 (NCH$_2$CH$_2$*C*H$_2$CH$_3$), 13.84 (NCH$_2$CH$_2$-CH$_2$*C*H$_3$). $^{31}P\{^1H\}$ NMR (CD_2Cl_2, 298 K): δ 17.43. Anal. Calcd for $C_{49}H_{49}BF_4IrN_3P_2$: C, 57.26; N, 4.17; H, 4.71. Found: C, 57.33; N, 4.20; H, 4.78.

(η^2-C,N)(*N*-Methyl-*N*′-(2-pyridylmethyl)imidazole-5-ylidene)bis-(hydrido)bis(triphenylphosphine)iridium(III) Hexafluoroantimoniate (3g). *N*-Methyl-*N*′-(2-pyridylmethyl)imidazolium hexafluoroantimoniate (33 mg, 0.080 mmol) and $IrH_5(PPh_3)_2$ (55 mg, 0.080 mmol) in THF (5 mL) were vigorously refluxed in air for 2 h. After the mixture was cooled to room temperature, 50 mL of pentane was added. A yellowish precipitate was filtered off and dried in vacuo. Yield: 71 mg (80%). Pure **3g** can be obtained by recrystallization from $CHCl_3$/pentane.

^1H NMR ($CDCl_3$, 298 K): δ 8.38 (s, 1H, NC*H*N), 8.22 (d, 1H, $^3J_{HH}$ = 5.5 Hz, py-*H*), 7.38−7.18 (m, 32H, py-*H*, ph-*H*), 6.10 (t, 1H, $^3J_{HH}$ = 6.6 Hz, py-*H*), 4.89 (s, 1H, im-*H*), 4.58 (s, 2H, C*H*$_2$), 3.38 (s, 3H, C*H*$_3$), −10.86 (dt, $^3J_{HH}$ = 5.0 Hz, $^2J_{PH}$ = 19.8 Hz, Ir-*H*), −21.53 (dt, $^3J_{HH}$ = 5.0 Hz, $^2J_{PH}$ = 18.6 Hz, Ir-*H*). $^{13}C\{^1H\}$ NMR ($CDCl_3$, 298 K): δ 161.97 (C_{py}), 153.22 (C_{py}), 142.43 (t, J_{PC} = 6.5 Hz, $C_{carbene}$), 137.23 (C_{py}), 134.87 (t, J_{PC} = 26.5, C_{ph}), 133.61 (t, J_{PC} = 6.3, C_{ph}), 133.39 (N*C*N), 129.65 (C_{ph}), 128.00 (C_{py}), 127.87 (t, J_{PC} = 4.8, C_{ph}), 125.50 (C_{im}), 124.21 (C_{py}), 55.36 (CH_2), 34.57 (CH_3). $^{31}P\{^1H\}$ NMR ($CDCl_3$, 298 K): δ 22.67. Anal. Calcd for $C_{46}H_{43}F_6IrN_3P_2Sb$·2$CHCl_3$: C, 45.26; H, 3.56; N, 3.37. Found: C, 45.55; H, 3.43; N, 3.55.

(η^2-C,N)(*N*-Isopropyl-*N*′-(2-pyridylmethyl)imidazole-5-ylidene)-bis(hydrido)-bis(triphenylphosphine)iridium(III) Tetrafluoroborate (3i). A mixture of *N*-isopropyl-*N*′-(2-pyridylmethyl)imidazolium tetrafluoroborate (40 mg, 0.140 mmol) and $IrH_5(PPh_3)_2$ (100 mg, 0.140 mmol) in THF (5 mL) was refluxed in air for 2 h. After 15 min, a clear solution was obtained. The yellow product precipitated by addition of 25 mL of pentane to the cooled mixture was filtered off and dried in vacuo. Yield: 120 mg (85%). The complex can be recrystallized from THF/pentane. Crystals of a quality suitable for X-ray analysis were obtained from CH_2Cl_2/Et_2O. ^1H NMR ($CDCl_3$, 298 K): δ 8.72 (s, 1H, NCHN), 8.23 (d, 1H, $^3J_{HH}$ = 5.5 Hz, H_{py}), 7.37−7.14 (m, 32H, H_{py}, H_{ph}), 6.07 (t, $^3J_{HH}$ = 6.3 Hz, H_{py}), 5.17 (s, 1H, H_{im}), 4.70 (s, 2H, CH_2), 4.25 (septet, 1H, $^3J_{HH}$ = 6.5 Hz, CH), 1.19 (d, 6H, $^3J_{HH}$ = 6.5 Hz, CH_3), −10.83 (dt, $^2J_{PH}$ = 19.6 Hz, $^3J_{HH}$ = 4.9 Hz, Ir-*H*), −21.49 (dt, $^2J_{PH}$ = 18.6 Hz, $^3J_{HH}$ = 4.9 Hz, Ir-*H*). $^{13}C\{^1H\}$ NMR ($CDCl_3$, 298 K): δ 161.78 (C_{py}), 153.10 (C_{py}), 141.07 (t, J_{PC} = 7.1 Hz, $C_{carbene}$), 137.04 (C_{py}), 134.93 (t, J_{PC} = 26.3 Hz, C_{ph}), 133.55 (t, J_{PC} = 6.0 Hz, C_{ph}), 132.40 (NCN), 129.55 (C_{ph}), 127.84 (t, J_{PC} = 5.8 Hz, C_{ph}), 125.87 (C_{py}), 124.15 (C_{py}), 123.56 (C_{im}), 55.03 (CH_2), 50.47 (CH), 22.94 (CH_3). $^{31}P\{^1H\}$ NMR ($CDCl_3$, 298 K): δ 21.36; mp = 246−248 °C (dec). Anal. Calcd for $C_{48}H_{47}BF_4IrN_3P_2$·THF: C, 57.88; H, 5.14; N, 3.89. Found: C, 57.84; H, 5.32; N, 3.74.

(η^2-C,N)(*N*-Butyl-*N*′-(2-pyridyl-methyl)imidazole-5-ylidene)bis-(hydrido)-bis(triphenylphosphine)iridium(III) Tetrafluoroborate (3j). A mixture of *N*-butyl-*N*′-(2-pyridylmethyl)imidazolium tetrafluoroborate (54 mg, 0.18 mmol) and $IrH_5(PPh_3)_2$ (129 mg, 0.18 mmol) in THF (8 mL) was refluxed in air for 2 h. After 20 min, a clear solution was obtained. The cooled reaction mixture was layered with heptane (10 mL). Over 12 h, crystals formed that were filtered off and dried in vacuo. Yield: 124 mg (68%). The complex can be recrystallized from THF/pentane. ^1H NMR ($CDCl_3$, 298 K): δ 8.71 (s, 1H, NCHN), 8.19 (d, 1H, $^3J_{HH}$ = 5.1 Hz, H_{py}), 7.37−7.15 (m, 32H, H_{py}, H_{ph}), 6.07 (t, $^3J_{HH}$ = 5.9 Hz, H_{py}), 5.03 (s, 1H, H_{im}), 4.72 (s, 2H, CH_2), 3.63 (t, 1H, $^3J_{HH}$ = 6.9 Hz, CH_2), 1.47 (m, 2H, CH_2), 1.17 (m, 2H, CH_2), 0.90 (t, $^3J_{HH}$ = 7.7 Hz, CH_3), −10.89 (dt, $^2J_{PH}$ = 19.6 Hz, $^3J_{HH}$ = 5.1 Hz, Ir-H), −19.61 (dt, $^2J_{PH}$ = 18.4 Hz, $^3J_{HH}$ = 5.1 Hz, Ir-H). $^{13}C\{^1H\}$ NMR ($CDCl_3$, 298 K): δ 161.77 (C_{py}), 153.07 (C_{py}), 141.30 (t, J_{PC} = 6.9 Hz, $C_{carbene}$), 137.09 (C_{py}), 134.96 (t, J_{PC} = 26.3 Hz, C_{ph}), 133.79 (NCN), 133.61 (t, J_{PC} = 6.0 Hz, C_{ph}), 129.59 (C_{ph}), 127.86 (t, J_{PC} = 4.7 Hz, C_{ph}), 126.13 (C_{im}), 125.90 (C_{py}), 124.18 (C_{py}), 55.08 (CH_2), 47.89 (CH_2),

31.96 (CH_2), 19.36 (CH_2), 13.37 (CH_3). $^{31}P\{^1H\}$ NMR ($CDCl_3$, 298 K): δ 21.39; mp = 229 °C (dec). Anal. Calcd for $C_{49}H_{49}BF_4IrN_3P_2$.THF: C, 58.24; H, 5.26; N, 3.84. Found: C, 58.23; H, 5.29 N, 3.90.

Anion Exchange: Method 2. This was typically carried out from the bromide salt with either the silver salt of the desired anion in CH_2Cl_2 or the sodium salt in acetone (1:1 molar ratio, 2 h, room temperature, stirring). AgBr or NaBr was removed by filtration, and the product was crystallized by addition of Et_2O. The outcome can be monitored by proton NMR using the CH proton at C2 as an indicator (**1** or **3**) or by ESI-MS. Occasionally, more than one exchange cycle was required for complete exchange.

Computational Details. All of the calculations have been performed with the Gaussian 98 package of programs.[53] The calculations on the structure and energetic of the ion-pairs were performed with the ONIOM method.[54] The experimental systems **2i** and **3i** were explicitly considered where the phenyl groups on PPh_3 and the ^{i}Pr group on N were treated at the UFF level,[55] and the remainder of the ion-pair, including the counteranion BF_4, Br, or OAc, was calculated at the B3PW91 level.[56,57] The energies of the ion-pair were calculated within the CPCM scheme[58,59] (CH_2Cl_2 as a solvent) on the ONIOM geometries, and the formation energy of the ion-pair was evaluated as $E_b = E(\text{ion-pair}) - \{E(\text{cation}) + E(\text{anion})\}$ where the energies are calculated at the CPCM level on frozen geometries for the fragments as obtained in the ONIOM calculations.

For the mechanistic study, the system considered was the *N*,*N*′-dialkyl-imidazolium salts (R = Me, R′ = Me; R = Me, R′ = ^{i}Pr; A = BF_4, Br) reacting with $IrH_3(PMe_3)_2$. The calculations have been performed at the B3PW91 level.

In all of the calculations throughout the paper, Ir, Br, and P were represented with the small core RECP from the Stuttgart's group and the associated basis set,[60,61] augmented by a polarization function.[62,63] The remaining atoms (C, H, N, B, F, O) were represented by a 6-31G-(d,p) basis set.[64] The nature of all of the extrema located has been determined after analytic calculations of the vibrational frequencies.

Acknowledgment. We thank the Université Montpellier 2 (O.E., E.C.), the CNRS (O.E., E.C.), the US DOE (A.K., J.R.M., A.R.C., R.H.C.), Johnson Mathey (L.N.A.), Ministero dell'Universitá e della Ricerca Scientifica e Tecnologica (MURST, Rome, Italy; A.M.), programma di Rilevante Interesse Nazionale, Cofinanziamento 2004-2005 (A.M.), and the COST D24/WG 0014/02 action (A.M., E.C.) for funding.

Supporting Information Available: A complete list of authors for ref 53; $^{19}F,^1H$-HOESY spectrum of **5** in CD_2Cl_2 (Figure S1); ^1H-NOESY spectra of **5** in CD_2Cl_2 (Figure S2) and CD_3NO_2 (Figure S3); $^{19}F,^1H$-HOESY spectra of **3j** and **2j** in CD_2Cl_2 (Figure S4); PGSE NMR data (Table S1); NPA charges and Wiberg bond indices (Table S2); and a full list of atomic Cartesian coordinates, energies (*E*, au), and free energies (*G*, au) for all computed systems. This material is available free of charge via the Internet http://pubs.acs.org.

JA055317J

(53) Pople, J. A.; et al. *Gaussian 98*; Gaussian, Inc.: Pittsburgh, PA, 1998.
(54) Svensson, M.; Humbel, S.; Froese, R. D. J.; Matsubara, T.; Sieber, S.; Morokuma, K. *J. Phys. Chem.* **1996**, *100*, 19357.
(55) Rappé, A. K.; Casewitt, C. J.; Colwell, K. S.; Goddard, W. A.; Skiff, W. M. *J. Am. Chem. Soc*. **1992**, *114*, 10024.
(56) Becke, A. D. *J. Chem. Phys.* **1993**, *98*, 5648.
(57) Perdew, J. P.; Wang, Y. *Phys. Rev. B* **1992**, *45*, 13244.
(58) Barone, V.; Cossi, M. *J. Phys. Chem. A* **1998**, *102*, 1995.
(59) Cossi, M.; Rega, N.; Scalmani, G.; Barone, V. *J. Comput. Chem.* **2003**, *24*, 669.
(60) Andrae, D.; Häussermann, U.; Dolg, M.; Stoll, H.; Preu*β*, H. *Theor. Chim. Acta* **1990**, *77*, 123.
(61) Bergner, A.; Dolg, M.; Küchle, W.; Stoll, H.; Preu*β*, H. *Mol. Phys*. **1993**, *30*, 1431.
(62) Ehlers, A. W.; Böhme, M.; Dapprich, S.; Gobbi, A.; Höllwarth, A.; Jonas, V.; Köhler, K. F.; Stegmann, R.; Veldkamp, A.; Frenking, G. *Chem. Phys. Lett.* **1993**, *208*, 111.
(63) Höllwarth, A.; Böhme, H.; Dapprich, S.; Ehlers, A. W.; Gobbi, A.; Jonas, V.; Köhler, K. F.; Stegmann, R.; Veldkamp, A.; Frenking, G. *Chem. Phys. Lett.* **1993**, *208*, 237.
(64) Hariharan, P. C.; Pople, J. A. *Theor. Chim. Acta* **1973**, *28*, 213.